frontiers | Frontiers in Earth Science

ORIGINAL RESEARCH
published: 11 April 2022
doi: 10.3389/feart.2022.866314

A Novel Tracer Technique to Quantify the Lithogenic Input Flux of Trace Elements to Qinghai Lake

Pu Zhang[1,2], Xuezheng Pei[2], Chenyang Cao[2], Chi Chen[1], Ziqin Gong[1], Xuerou Li[1], Jingya Pang[1], Lihua Liang[2], Xiangzhong Li[3]*, Youfeng Ning[1] and R.Lawrence Edwards[4]*

[1]Institute of Global Environmental Change, Xi'an Jiao Tong University, Xi'an, China, [2]College of Urban and Environmental Sciences, Northwest University, Xi'an, China, [3]Yunnan Key Laboratory of Earth System Science, Yunnan University, Kunming, China, [4]Department of Earth and Environmental Sciences, University of Minnesota, Minneapolis, MN, United States

OPEN ACCESS

Edited by:
Mao-Yong He,
Institute of Earth Environment (CAS), China

Reviewed by:
Yibo Yang,
Institute of Tibetan Plateau Research (CAS), China
Dejun Wan,
Nantong University, China
Junsheng Nie,
Lanzhou University, China

***Correspondence:**
Pu Zhang
zhangpu357@xjtu.edu.cn
Xiangzhong Li
xzhli04@163.com

Specialty section:
This article was submitted to Geochemistry, a section of the journal Frontiers in Earth Science

Received: 31 January 2022
Accepted: 15 March 2022
Published: 11 April 2022

Citation:
Zhang P, Pei X, Cao C, Chen C, Gong Z, Li X, Pang J, Liang L, Li X, Ning Y and Edwards RL (2022) A Novel Tracer Technique to Quantify the Lithogenic Input Flux of Trace Elements to Qinghai Lake. Front. Earth Sci. 10:866314. doi: 10.3389/feart.2022.866314

Thorium (Th) isotopes were applied to quantify the contributions of lithogenic inputs to the Qinghai Lake (QHH). Concentrations of dissolved ^{232}Th and ^{230}Th were measured in 59 water samples collected from Qinghai Lake and its exogenous recharge rivers. There are significant differences in the concentration of ^{232}Th of the sampled water in QHH that confirm the input of variable lithogenic material sources. The ^{230}Th concentrations were used to calculate a scavenging residence time for Th, which was then applied to calculate the flux of dissolved ^{232}Th by matching the measured concentrations of dissolved ^{232}Th. Then the ^{232}Th content of lithogenic material was used with the solubility of Th from the preliminary particle data from the Qinghai–Qaidam district. When using a Th solubility from particles of 1%, the fluxes of lithogenic material range from 0.03 to 25.25 g/m^2/yr in the surface water, consistent with the flux results of settled particles from the previous study. When a large number of exogenous recharge rivers are mixed into the northwest basin of Qinghai Lake, the ^{232}Th content and lithogenic flux of the lake water are mainly influenced by the type and content of the particles in the Buha and Shaliu rivers. Conversely, in south basin with limited recharging rivers, the ^{232}Th content of the lake water away from the estuary is mainly influenced by atmospheric dust. Furthermore, based on the ^{230}Th normalization method (combining with ^{232}Th and τ_{Th}), the Buha and Shaliu rivers located in the northwest basin contribute about 90% of the detrital flux to the lake. The lithogenic flux in the southeast lake is dominated by dust flux with a value of ~0.109 g/m^2/yr, while the higher lithogenic flux at the bottom of the lake was likely generated by accumulated sinking particulate matter and resuspension of bottom sediments in September. This study confirms the utility of long-lived Th isotopes to quantify lithogenic inputs based on the Th content of the dissolved lake water and also supply deposition resolution information for QHH sediment records with some certainty.

Keywords: ^{232}Th content, ^{230}Th normalization technique, lithogenic flux, dust flux, Qinghai Lake

INTRODUCTION

As an important component of atmospheric aerosols, dust has a significant impact on the Earth's climate system, biogeochemical cycle, water cycle, and human health. Dust plays a role in different components of the climate by influencing the radiative balance and thus the energy balance of the Earth's system. Dust can also act as cloud condensation nuclei, altering the hydrological cycle by changing cloud cover and microphysics (Jickells et al., 2005; Ding et al., 2009). The dust cycle is an important component of the Earth system, and the arid and semi-arid zones of Central Asia are one of the key regions for global change research due to their vast area and the huge amount of dust they provide (800 Tg of dust is delivered to the atmosphere each year in northwest China alone; Zhang et al., 1997). In addition, dust can also act as an exogenous source of nutrients to marine and remote terrestrial ecosystems, participating in carbon cycle processes (Martin and Fitzwater, 1988; Jickells et al., 2005). In recent years, the mechanisms of dust release and transport have become a hot topic of interest for both modern climatology and paleoclimatology. In this regard, changes in dust fluxes not only depend on regional climate changes but also can influence them in various ways, thus making dust fluxes one of the key elements in the exploration of regional climate environments (Cruz et al., 2021).

The traditional approach to calculating lake burial fluxes relies on determining the average mass accumulation rates based on age model tie points, intervening sediment thickness, and average sediment dry bulk density (Lyle and Dymond, 1976; DeMaster, 1981; Curry and Lohmann, 1986; Lyle et al., 1988; Rea and Leinen, 1988; Sarnthein et al., 1988; Mortlock et al., 1991). The temporal resolution of this approach is limited by the robustness of the age model, including the number of chronological tie points and their associated errors (Francois et al., 2004). Furthermore, this approach can easily be biased by sediment redistribution on the edge of the lake with river input, where sediment transport from the river can exceed the vertical rain of particles from the water column. As a result, constant flux proxies such as the ^{230}Th normalization technique have the potential to be developed, providing more robust estimates of mass accumulation in the lake sediment. Constant flux proxies are geochemical parameters with well-constrained and stable source functions, such as ^{230}Th (Bacon, 1984; Francois et al., 2004) and ^{3}He (Marcantonio et al., 1996; Winckler et al., 2004; McGee and Mukhopadhyay, 2013). The U concentration of saline lakes in the alpine arid background is stable (Zhang et al., 2019; Zhao et al., 2020; Zhang et al., 2021). Furthermore, ^{230}Th is produced by the steady decay of uranium dissolved in lake water, after which it is rapidly eliminated by sinking particles and buried by the lake sediment (Francois et al., 2004; Zhang et al., 2019). Because the ^{230}Th production rate is relatively uniform in space and time, variability in ^{230}Th concentrations in the sediment can be theoretically attributed to variable dilution by changes in sediment mass flux over time. This technique, ^{230}Th normalization, allows both high-resolution sediment mass flux reconstructions independent of age model tie points and isolation of only the vertical component of sedimentation, regardless of the amount of lateral sediment transport from rivers.

The different isotopes of Th provide important information about the various processes occurring in the ocean. In seawater, Th has a stable IV oxidation state, which makes it highly particle reactive (Santschi et al., 2006); readily transports from the water column to particulate matter; and is buried in the underlying sediments as the particulate matter settles (Bourdon et al., 2003). Th isotopes have a very limited source in the lake environment, in which ^{232}Th accounts for about 99.98% of all natural Th isotopes, and it is obtained almost exclusively through dissolution of river, wind, and lake sediments (Krishnaswami and Cochran, 2016), while ^{234}Th, ^{230}Th, and ^{228}Th are derived from the α radioactive decay of ^{238}U, ^{234}U, and ^{228}Ra in the ocean, respectively (Ojovan and Lee, 2014). The production rates of ^{234}Th and ^{230}Th have remained essentially stable since the reserves of U nuclides and their isotopic compositions in the saline have remained essentially stable over years (Zhang et al., 2019). The combination of particle reactivity and constrained sources makes Th isotopes one of the most versatile tools for studying particle fluxes in the ocean and sedimentary record (Costa and McManus, 2017). Under stable conditions, the residence time of Th was obtained based on the production rate of ^{232}Th in the water column. The residence time combined with the storage of ^{230}Th obtained the flux of ^{232}Th (e.g., the ^{230}Th normalization technique), which in turn was extrapolated to the flux of terrestrial or atmospheric deposition (Hayes et al., 2013).

The Qinghai–Tibet Plateau in the midlatitudes is the largest plateau in the world with the highest average altitude and is sensitive to global climate change due to the interplay of westerly winds and Asian summer winds, as well as feedbacks to atmospheric circulation and hydrological processes in the surrounding areas. Therefore, it has received much attention from researchers, and its concept as the "third pole of the earth" has been widely accepted. There are many lakes on the Qinghai–Tibet Plateau, and many of them record rich information on environmental changes at different spatial and temporal scales and are windows for research on past environmental changes. The Qinghai Lake basin is located at the confluence of the eastern monsoon region of China, the northwest arid region, and the alpine region of the Qinghai–Tibet Plateau, with distinct regional climatic characteristics, and is one of the most sensitive areas to global climate change, playing a crucial role in maintaining the regional hydrological cycle. With the expansion and in-depth study of the sedimentary environment of Qinghai Lake, more and more discussions have been made on the depositional flux or rate. However, due to the different methods or sampling points, the deposition fluxes obtained by different researchers vary greatly (Jin et al., 2009a; Xu et al., 2010; Wan et al., 2012). Little attempt has been made to define the chemical budget and mass balance of the $CaCO_3$-rich sediments in Lake Qinghai, which are the basis of paleoenvironmental and paleoclimatic reconstructions using lake sediments. The results from the Lake Qinghai River system in the northeastern Tibetan Plateau suggest that atmospheric dust contributes 36–57% of the total dissolved cations to the river waters and further into Qinghai Lake (Zhang et al., 2009).

Previous studies have confirmed that the contribution of atmospheric dust input to the elemental reservoir of Lake Qinghai water is up to about 65% based on the suspended particulate matter of the Buha River (Jin et al., 2009a). The soluble element content of lake waters is controlled by the variation of the elemental content of exogenously recharged river waters (Jin et al., 2009b). For studying the input–output budget characteristics, Qinghai Lake is uniquely positioned geographically to quantify the flux of Th and explore its potential to respond to environmental changes, thus providing more basic research information for subsequent evaluation of whether the U-series disequilibrium characteristics of lake sediments can provide the basin's paleo-weathering history.

In view of this, the study first attempts to obtain the water residence time of Qinghai Lake by assessing the ^{230}Th–^{234}U disequilibrium; second, by investigating the surface distribution characteristics of ^{232}Th concentration in the lake water column of Qinghai Lake and the recharging river and water column of the entire lake transect, we try to explore the source of ^{232}Th and the variation of lithogenic flux in the water column of Qinghai Lake, and understand its potential to the response of the environmental changes. To a certain extent, this will fill the gap in the revenue and expenditure characteristics of ^{230}Th and ^{232}Th and their geochemical significance in the lake domain and also be an important reference for understanding the ^{230}Th-indicated paleo-oceanic processes in marine sediments.

MATERIALS AND METHODS

Sampling Locations

Qinghai Lake (36°32′–37°15′N; 99°36′–100°47′E) is located in the northeastern part of the Qinghai–Tibet Plateau, with a length of about 109 km from east to west and a width of about 39.8 km from north to south, and an average water depth of 18.3 m. It is the largest inland saline lake in China. The geological and geographical environment and the current climate of this area have been examined in detail by Colman et al. (2007) and Jin et al. (2010). Qinghai Lake is developed within a basin surrounded by three mountain ranges, including Datong Mountain to the north, Riyue Mountain to the east, and the Qinghai Nanshan Mountains to the south (Bian et al., 2000). The lake is divided into two nearly equal sub-basins by an NNW-trending horst, from which an island (Mt. Haixin) emerges. Several minor fault scarps can also be found in the lake basin. The lake bed is generally flat, and the lake is hydrologically closed and evaporative (Zhang et al., 1994). The six largest rivers on the order of discharge inside the Lake Qinghai catchment are Buha, Shaliu, Hargai, Quanji, Daotang, and Heima rivers. These rivers are greatly impacted by the hydrological cycle linked to the area's monsoonal climate, and they supply over 87% of the water (Li et al., 2007), ~67% of the dissolved load (Jin et al., 2009a), and sediment discharge to the lake. Over half of these rivers start from the Buha River, whose water chemistry is affected by the underlain marine limestone and sandstones, which constrain carbonate-dominated compositions of the lake water (Jin et al., 2009b). Meltwater from surrounding mountain glaciers accounts for only 0.3% of the total runoff (Colman et al., 2007).

Qinghai Lake is a typically closed saline lake, and there is no output of surface water from the lake. The lake's recharge water is mainly the recharging rivers, followed by natural precipitation and groundwater. There are more than 70 rivers of various sizes flowing into the lake, with an obvious asymmetrical distribution, the northwestern part being relatively large and having a high runoff volume, while the southeastern part is sparse and mostly seasonal. The runoff of the rivers is unevenly distributed within the year, with July to September having the highest runoff, accounting for 60%–80% of the total annual runoff, and January to February has the lowest runoff, accounting for only about 1% of the total annual runoff. Qinghai Lake receives its annual runoff recharge mainly from seven rivers, including the Buha, Shaliu, Hargai, Quanji, Ganzi, Daotang, and Heima rivers. The total annual runoff is about 2.5 billion m^3, and the main rivers have a total annual runoff of about 2.2 billion m^3, accounting for 90% of the total runoff in the basin.

The Buha River is the largest exogenous recharge river in the Qinghai Lake basin, with a total length of 286 km, a basin area of 14,387 km^2, an average multi-year runoff of 7.85×10^8 m^3, and a contribution of 46.9% of the runoff into the lake. The Shaliu River is the second largest recharge river in the Qinghai Lake basin, with a total length of about 106 km and a basin area of 1, 500 km^2, with an average annual runoff of 2.46×10^8 m^3, accounting for 14.5% of the total runoff into the lake. The third largest recharge river in the basin is the Hargai River. The Buha River, Shaliu River, and Hargai River account for more than 75% of the total runoff into the lake. Apart from these, the rest of the recharge rivers are relatively small in terms of basin area and average annual runoff and are mostly seasonal rivers that dry up seasonally (the Quanji River is 65 km long and has a basin area of 567 km^2, the Daotang River is 60 km long and has a basin area of 727 km^2, the Heima River is 17.2 km long and has a basin area of 107 km^2, and the Ganzi River does not directly drain into Qinghai Lake but is surface runoff, which is submerged underground and then partly fed into the lake as groundwater). It is worth noting that the Daotang River is the only river in the Qinghai Lake basin that flows in a southeast to northwest direction.

Sampling Design and Methods

The water samples collected include Qinghai Lake and its exogenous recharge rivers. Among the recharge rivers, the Buha River, Shaliu River, Hargai River, and Daotang River were selected as the main study areas in view of the influence of various factors, such as the contribution rate of runoff from exogenous recharge rivers, the lithology control of the basins, and the seasonal differences of rivers. Due to the lack of seasonal water during the sampling period, no samples were collected from the Quanji River or the Heima River.

A sampling of the water samples required for the study continued from 2017 to 2020 and can be divided into four batches. In the first sampling batch, water samples were collected from Qinghai Lake in September 2017. The subsequent batches mainly sampled the duplicate samples from Qinghai Lake and the water samples from the exogenous

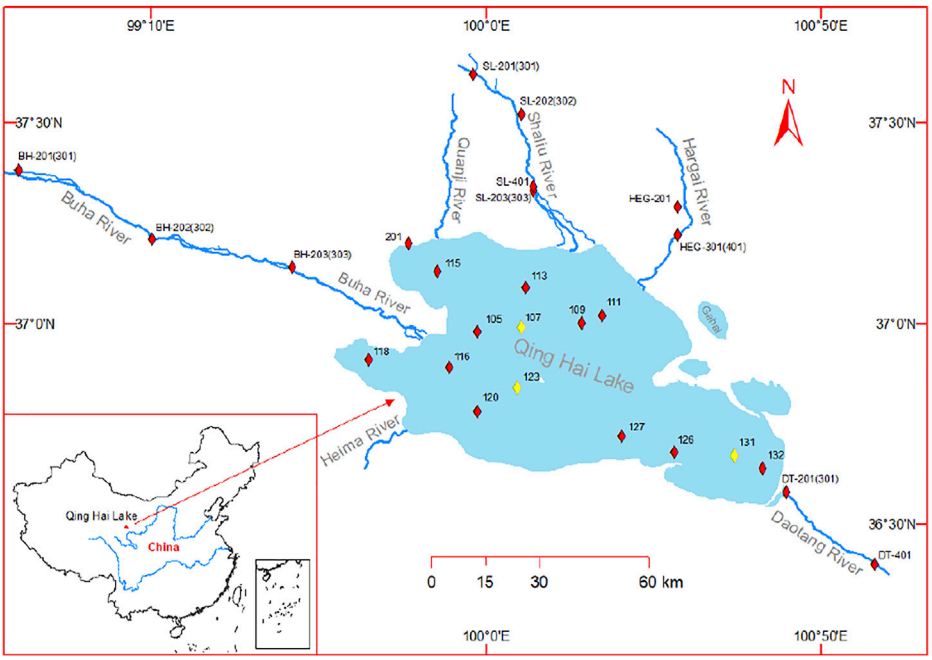

FIGURE 1 | Map showing the locations of the sampled lakes and rivers in the Qinghai region. (Red diamonds represent surface sites and yellow diamonds represent depth profiles).

recharge rivers of Qinghai Lake in June 2018, August 2019, and November 2020.

In the first batch, a total of 14 sampling sites were set up to sample the waters of Qinghai Lake, with a sampling range of 36°38′25″~37°07′52″N, 99°42′48″~100°41′23″E. Among them, three sampling sites took water samples from the surface layer (~0.2 m) to the bottom layer of the lake at 3-m intervals, while the remaining nine sampling sites collected water samples from the surface layer of the lake only. One surface water sample was also taken during the second batch of sampling, and a total of 40 samples were collected from Qinghai Lake. The second, third, and fourth batches of water samples were collected from the exogenous recharge rivers of Qinghai Lake, including 13 samples from the upper, middle, and lower reaches of the Buha River and Shaliu River (6 from the Buha River and 7 from the Shaliu River), while six samples were collected from the Hargai River and Daotang River (3 from the Hargai River and 3 from the Daotang River), which are near the entrance of the rivers. A total of 19 samples were collected from the recharge rivers. The distribution of the sampling sites is shown in **Figure 1**.

Surface water samples from Qinghai Lake and its exogenous recharge rivers were collected directly in high-density polyethylene (HDPE) plastic bottles, while other water samples at different depths were collected in HDPE plastic bottles using a Plexiglas (PPMA) water collector. The first batch of 39 water samples collected from Qinghai Lake in September 2017 were transferred to a 50 ml centrifuge tube and centrifuged three times (7 min) at 3,500 rpm to remove insoluble impurities such as insoluble particles. After centrifugation, the supernatant of each sample was taken and stored in a new HDPE plastic bottle to analyze the follow-up chemistry procedure. Samples collected from the other batches were filtered within 24 h of collection using a Nalgene manual vacuum filtration system (Nalgene 300–4,100; 6,133–0,010) with a 0.8-μm pore size mixed cellulose membrane (Millipore AAWP04700). After pretreatment, the water samples were stored in HDPE plastic bottles and sent to the laboratory for testing. The details of sampling information are shown in **Table 1**.

In order to verify whether centrifugation and filtration methods to separate particles affect the experimental results, three samples were centrifuged and filtered through 41-, 0.8-, and 0.45-μm filters, respectively, to assess the proportion of particulate matter of different sizes in the total particulate matter. The results show that the particle sizes in the centrifuged samples were less than 41 μm. In addition, we compared ^{232}Th concentrations filtered by 41-μm filters and 0.8-μm filters in four lakes from the Qaidam Basin (**Table 2**). The results show that the size of thorium-enriched particles is mostly between 0.8 and 41 μm, and the proportion of particles less than 0.8 μm is limited. Thus, the lake fluxes involved in this study are calculated from the ^{232}Th concentration in a particulate matter less than 41 μm, and the ^{232}Th concentration in river waters is in a particulate matter less than 0.8 μm. Therefore, we believe that Th concentration filtered by 0.8-μm filters and centrifugation three times could represent the content of dissolved Th in saline lake water to a certain extent.

The method of Th isotope analysis of water samples can be broadly divided into two stages: chemical separation and mass spectrometry, where the chemical separation stage consists of co-precipitation, low-speed centrifugation, ion-exchange resin

TABLE 1 | Sampling site information for the water samples.

Location	Sample no.	Depth (m)	Station	Latitude (°N) and longitude (°E)	Date	Batch
Qinghai Lake	QHH-9-0	0.2	107	36°59′35″, 100°05′22″	10 September 2017	1
	QHH-9-3	3				
	QHH-9-6	6				
	QHH-9-9	9				
	QHH-9-12	12				
	QHH-9-15	15				
	QHH-9-18	18				
	QHH-9-21	21				
	QHH-9-24	24				
	QHH-9-27	27				
	QHH-15-0	0.2	123	36°50′12″, 100°04′59″	11 September 2017	1
	QHH-15-3	3				
	QHH-15-6	6				
	QHH-15-9	9				
	QHH-15-12	12				
	QHH-15-18	18				
	QHH-15-21	21				
	QHH-15-27	27				
	QHH-21-0	0.2	131	36°39′59″, 100°37′18″	17 September 2017	1
	QHH-21-3	3				
	QHH-21-6	6				
	QHH-21-9	9				
	QHH-21-12	12				
	QHH-21-15	15				
	QHH-21-18	18				
	QHH-21-21	21				
	QHH-21-24	24				
	QHH-21-26	26				
	QHH-105-S	0.2	105	36°59′05″, 99°58′41″	10 September 2017	1
	QHH-109-S	0.2	109	36°54′45″, 100°14′06″	10 September 2017	1
	QHH-111-S	0.2	111	37°00′56″, 100°17′19″	10 September 2017	1
	QHH-113-S	0.2	113	37°05′12″, 100°05′56″	10 September 2017	1
	QHH-115-S	0.2	115	37°07′52″, 99°53′03″	10 September 2017	1
	QHH-116-S	0.2	116	36°53′15″, 99°54′46″	11 September 2017	1
	QHH-118-S	0.2	118	36°54′23″, 99°42′48″	11 September 2017	1
	QHH-120-S	0.2	120	36°46′34″, 99°59′02″	11 September 2017	1
	QHH-126-S	0.2	126	36°40′41″, 100°28′09″	17 September 2017	1
	QHH-127-S	0.2	127	36°43′19″, 100°20′18″	17 September 2017	1
	QHH-132-S	0.2	132	36°38′25″, 100°41′32″	17 September 2017	1
	QHH-201-S	0.2	201	37°11′52″, 99°48′34″	18 June 2018	2
Buha River	BH-201	0.2	201	37°22′35″, 98°50′34″	17 June 2018	2
	BH-202	0.2	202	37°12′53″, 99°09′54″	17 June 2018	2
	BH-203	0.2	203	37°08′06″, 99°30′59″	17 June 2018	2
	BH-301	0.2	301	37°22′35″, 98°50′34″	23 July 2019	3
	BH-302	0.2	302	37°12′53″, 99°09′54″	23 July 2019	3
	BH-303	0.2	303	37°08′06″, 99°30′59″	23 July 2019	3
Shaliu River	SL-201	0.2	201	37°37′18″, 99°58′17″	18 June 2018	2
	SL-202	0.2	202	37°31′09″, 100°05′11″	18 June 2018	2
	SL-203	0.2	203	37°19′43″, 100°07′28″	18 June 2018	2
	SL-301	0.2	301	37°37′18″, 99°58′17″	23 July 2019	3
	SL-302	0.2	302	37°31′09″, 100°05′11″	23 July 2019	3
	SL-303	0.2	303	37°19′43″, 100°07′28″	23 July 2019	3
	SL-401	0.2	401	37°19′92″, 100°07′29″	18 November 2020	4
Hargai River	HEG-201	0.2	201	37°17′11″, 100°28′38″	18 June 2018	2
	HEG-301	0.2	301	37°13′11″, 100°28′37″	23 July 2019	3
	HEG-401	0.2	401	37°13′11″, 100°28′39″	18 November 2020	4
Daotang River	DT-201	0.2	201	36°34′30″, 100°44′49″	19 June 2018	2
	DT-301	0.2	301	36°34′30″, 100°44′49″	24 July 2019	3
	DT-401	0.2	401	36°23′56″, 100°58′28″	18 November 2020	4

TABLE 2 | ^{232}Th concentration of samples filtered by 41-μm and 0.8-μm filters from several lakes in the Qaidam Basin.

Location	Sample	Latitude (°N) and longitude (°E)	^{232}Th (pmol/kg)	Error (2s)	Filter (μm)	Date
Qinghai Lake	QHH-4	37°02′54″,100°26′52″	326.553	5.39	41	2021/2/26
	QHH-4-F		2.046	0.01	0.8	
Qinghaigahai Lake	QHGH-2	37°01′19″,100°35′40″	41.792	0.26	41	2021/2/26
	QHGH-2-F		3.094	0.02	0.8	
Xiligou Lake	XLGH-6	36°49′05″,98°27′21″	65.287	0.52	41	2021/2/26
	XLGH-6-F		3.239	0.04	0.8	
Gahai Lake	GH-8	37°06′53″,97°36′07″	263.454	4.03	41	2021/2/26
	GH-8-F		0.340	0.00	0.8	

separation, collection, and purification. The specific steps involved are as follows:

1) Co-precipitation separation: A certain amount of water sample was weighed in a pre-prepared HDPE plastic bottle, a certain amount of 14N HNO_3 (1 N = 1 M), and 1–2 drops of $HClO_4$ and tracer (^{233}U–^{236}U–^{229}Th) were added to the water sample, heated and dried, and 2N HCl was used to dissolve the dried sample. Then, three to five drops of Fe solution was added to the sample, use $NH_3{\cdot}H_2O$ to reconcile the pH of the sample to 8 to 9, and mixed well and left for some time until a yellow precipitate appears at the bottom of the bottle.
2) Low-speed centrifugation: The water sample was transferred into a centrifuge tube and centrifuged at a low speed. After skimming off the upper clear layer, the resulting iron salt precipitate was rinsed with ultrapure water (>18 MΩ). The centrifugation process can be repeated 2–3 times to avoid other metal ions and soluble impurities from affecting the results. The resulting iron salt precipitate was dissolved by 14N HNO_3, transferred to a Teflon beaker, and then heated and dried for the next treatment.
3) Ion-exchange resin separation: The precipitate was completely dissolved using 7N HNO_3 and then transferred to a pre-prepared AG1-X8 anion resin exchange column, followed by the addition of 3CV 7N HNO_3 to remove Fe (CV: column volume), 3CV 6N HCl to achieve the Th isotope separation process.
4) Collection and purification: For this, 1 to 2 drops of $HClO_4$ was added to the separated Th isotope solution, heated and dried, and then dissolved with 14N HNO_3. The procedure was repeated 2–3 times, then fixed using a dilute acid (2% HNO_3 + 0.01% HF), and transferred to a small plastic vial for subsequent mass spectrometric analysis.

The mass spectrometry procedure was relatively straightforward. The nuclide ratio of samples was determined by Thermo Fisher's Neptune Plus MC-ICP-MS, and the concentrations of ^{230}Th and ^{232}Th in samples were calculated by isotope dilution. All measurements were carried out using the peak jump program in ion counting mode at the retarding potential quadruple. For Th, the measurement uncertainties involved propagated errors from ICP-MS isotope ratio measurements, spike concentrations, and blank corrections. The procedural blanks for chemical and mass spectrometric analyses at the Laboratory of Isotope Geochemistry in Xi'an Jiao Tong University are approximately 205 fg (5.3 e^6 atoms) for ^{232}Th, and 37 ag (1.0 e^5 atoms) for ^{230}Th. The methods used herein have been fully described by Cheng et al. (2000), Cheng et al. (2013) and Shen et al. (2002), Shen et al. (2012).

The measured ^{230}Th concentrations were corrected for in-growth due to decay of ^{234}U throughout the time the specimen was retained. To utilize ^{230}Th-^{234}U disequilibrium to obtain a Th residence time, ^{230}Thxs concentrations must also be corrected for the proportion of ^{230}Th liberated by the dissolution of lithogenic substances. This adjustment is made with concurrent measurements of ^{232}Th, with a lithogenic ratio of ^{230}Th/^{232}Th = 4.0×10^{-6} mol/mol (Roy-Barman et al., 2009).

Theory

The particle-reactive isotopes in the U and Th decay series are helpful tracers of particulate flux in water. The geochemistry of ^{230}Th in sediments is also important with respect to spatial and temporal variations in particulate flux (Ankney et al., 2017). Previous studies have shown that ^{230}Th is produced by the decay of ^{234}U at a constant rate. In natural waters, ^{230}Th is adsorbed by particulate matter in the water and eliminated from the water as it sinks. This process takes much less time than its radioactive decay rate (half-life of ^{232}Th = 14.1×10^9 years; half-life of ^{230}Th = 75.6×10^3 years) (Edmonds et al., 2004). The scavenging rate of Th is equal to the reciprocal of its corresponding residence time, and the hydraulic residence time of Th (τ_{Th}) in the lake water column can be obtained by measuring the concentration of ^{230}Thxs in water (**Eq. 1**) (Hayes et al., 2013).

$$\tau Th(z) = \frac{\int_0^z dissolved^{230}Thxs dz}{\int_0^z activity^{234}U \times \lambda_{230} dz} \quad (1)$$

where the multiplication of ^{234}U activity and λ_{230} is considered as the increment of ^{230}Th, $\lambda_{230} = 9.1705 \times 10^{-6}$ (Cheng et al., 2013).

In the following, the ^{232}Th fluxes will be calculated, and their contributions will be assessed in relation to the ^{232}Th distribution characteristics of the lake water column, respectively. The formula for calculating the ^{232}Th fluxes in lake water is given in **Equation 2** (Hayes et al., 2013).

$$dissolved^{232}Thflux(z) = \frac{\int_0^z d^{232}Thdz \times \int_0^z (\lambda_{230}^{234}U)dz}{\int_0^z d^{230}Thxsdz} = \frac{\int_0^z d^{232}Thdz}{\tau Th} \quad (2)$$

The dissolved ^{232}Th flux was then used to estimate a particulate lithogenic flux considering the content of ^{232}Th in the basaltic lithogenic material around the QHH region (10.5 μg/g; Wang et al., 2016) and the fractional solubility of ^{232}Th in lithogenic material (S_{Th}; from our preliminary Th result of particles from QHH and Qaidam Basin) as shown in **Equation 3** (Hayes et al., 2013).

$$Lithogenic\ flux(z) = \frac{Dissloved^{232}Th\ flux\ (z)}{[Th]_{QHH} \times S_{Th}} \quad (3)$$

To obtain an estimation of the flux of lithogenic material using dissolved Th-isotopes, it is first necessary to convert ^{232}Th concentrations into a dissolved flux using the residence time calculated. For this, dissolved ^{232}Th was integrated from the surface to an integration depth and divided by the corresponding ^{230}Th residence time (**Eq. (1)**).

RESULTS

The Spatial Distribution of Th Isotope Concentration in Surface Lake Water

Based on the surface water samples obtained from 15 different sampling locations in Qinghai Lake, the spatial distribution of Th isotope concentration data in the lake water is shown in Zhang et al. (2019). The details are shown in **Supplementary Table S1**. There are differences in the distribution of ^{232}Th concentrations between different sampling sites at the same depth, ranging from 0.265 to 3.356 pmol/kg, with a mean value of 1.247 pmol/kg, with the maximum value occurring at 107 and the minimum value at 131. The details are shown in the supplementary material file as **Supplementary Figure S1**. The total dissolved ^{230}Th concentration varied from 0.27 to 19.03 μBq/kg, with a mean value of 7.76 μBq/kg, with the maximum value occurring at site 127 and the minimum value at site 123, which fluctuated considerably. In the lake surface water, the ^{230}Thxs content of the 14 sites ranges from 0.2 to 18.2 μBq/kg with an average value of 7.39 μBq/kg, except for site 123, where no excess ^{230}Th occurred in the surface water. The maximum value appeared at site 127 and the minimum value appeared at site 201, with a large fluctuation and an average value of 7.39 μBq/kg.

In summary, there are significant differences in the concentrations of ^{232}Th, ^{230}Th, and ^{230}Thxs in the surface water of Qinghai Lake. The concentration of ^{232}Th at sites 107, 115, 116, 118, and 201, located at the edge of the northwest lake area, had significantly higher levels than other areas of the lake, with a mean value of 2.513 pmol/kg at the five sites, which was higher than the other samples. In contrast, the average content of ^{230}Thxs in sites 131, 126, 127, and 132 in the south lake area was 11.98 μBq/kg, far higher than the average value of surface water.

The Vertical Distribution of Th Isotope Concentrations in Lake Water

Lake water was sampled at varying depths at three sites (107, 123, and 131) in Qinghai Lake, and the results are shown in Zhang et al. (2019). The details are shown in **Supplementary Table S2**, **Supplementary Figure S2**, and **Supplementary Figure S3**. Site 107 is located in the northern lake area. The concentration of ^{232}Th varied from 3.356 to 14.995 pmol/kg, with an average value of 6.273 pmol/kg. From the surface to the bottom of the lake, the concentration of ^{232}Th exhibited a gradual and limited downward increase before decreasing at the bottom of the profile. Total dissolved ^{230}Th ranges from 7.08 to 21.59 μBq/kg, with an average value of 12.63 μBq/kg, with a maximum value at 21 m and a minimum value at 9 m. The concentration of ^{230}Thxs ranges from 5.3 to 12.5 μBq/kg, with a mean value of 8.24 μBq/kg, maximum values at 15 m and 27 m, and a minimum value at 9 m. The total dissolved ^{230}Th and ^{230}Thxs increased with depth before decreasing at a depth of 24 m.

At site 123, the concentration of ^{232}Th varied from 0.439 to 1.791 pmol/kg, with an average value of 1.005 pmol/kg. From the top to the bottom of the sampling profile, the concentration of ^{232}Th increased slightly with depth before decreasing at 21 m. The total dissolved ^{230}Th content ranges from 0.07 to 3.44 μBq/kg, with an average value of 1.35 μBq/kg, a maximum value at 21 m, and a minimum value at 3 m. The concentration of ^{230}Thxs content ranges from 0.5 to 2.2 μBq/kg, with a mean value of 1.16 μBq/kg. The maximum value occurs at 21 m and the minimum at 26 m.

At site 131, which is located in the southern lake area, the concentration of ^{232}Th ranged from 0.265 to 4.563 pmol/kg, which increased with the sampling depth, peaked at 21 m and then decreased, with an average value of 0.872 pmol/kg, lower than that of sites 123 and 107. The concentration of total dissolved ^{230}Th ranges from 7.34 to 18.61 μBq/kg, with an average value of 12.52 μBq/kg. The concentration of ^{230}Thxs ranges from 6.9 to 18.5 μBq/kg, with a mean value of 11.9 μBq/kg. The maximum and minimum values of total dissolved ^{230}Th and ^{230}Thxs occurred at 18m and 3m, respectively. Unlike sites 107 and 123, the concentration of total dissolved ^{230}Th and ^{230}Thxs in site 131 fluctuated widely and showed an overall decreasing trend with increasing depth.

Characteristics of Th Isotope Concentration Distribution in Exogenous Recharged River Waters

Overall, 19 surface water samples were sampled from the Buha River, Shaliu River, Hargai River, and Daotang River. The characteristics of the distribution of Th isotope concentration in these recharged river waters are shown in **Table 3**.

In the Buha River, the concentration of ^{232}Th ranges from 1.531 to 2.874 pmol/kg, with a mean value of 2.583 pmol/kg,

TABLE 3 | Distribution of Th isotope concentrations in exogenous recharge river water.

Sample no.	Depth (m)	$d^{234}U^*$ (Measured)	$d^{232}Th$ (pmol/kg)	$d^{230}Th$ (pmol/kg)	$d^{230}Th$ (μBq/kg)	$d^{230}Thxs$ (μBq/kg)
BH-201	0.2	902.1	3.354	1.81E-05	3.16	0.8
BH-202		934.2	2.861	2.06E-05	3.60	1.6
BH-203		1,194.8	2.36	1.90E-05	3.32	1.7
BH-301		1,017	1.531	4.13E-06	0.72	—
BH-302		1,031.8	2.874	1.06E-05	1.85	—
BH-303		1,066.2	2.518	9.23E-06	1.61	—
SL-201	0.2	1,087.7	7.976	5.30E-05	9.26	3.7
SL-202		1,148.6	7.904	5.27E-05	9.21	3.7
SL-203		1,203.3	7.530	4.96E-05	8.67	3.4
SL-301		1,279.0	4.488	2.16E-05	3.77	0.6
SL-302		898.6	7.773	3.82E-05	6.67	1.2
SL-303		1,213.0	3.800	1.80E-05	3.15	0.5
SL-401		1,325.1	46.913	2.28E-04	39.84	7.1
HEG-201	0.2	1,506.2	2.321	1.65E-05	2.88	1.3
HEG-301		1,295.2	3.132	1.50E-05	2.62	0.4
HEG-401		1,297.3	0.433	5.06E-04	88.41	88.1
DT-201	0.2	983.7	2.350	5.80E-04	101.34	99.7
DT-301		926.9	9.306	5.74E-05	10.03	3.5
DT-401		1,009.8	61.941	2.86E-04	49.97	6.7

showing a decreasing trend from the northwest (upstream) to southeast (downstream) regions. The concentration of total dissolved ^{230}Th ranges from 0.72 to 3.60 μBq/kg, with an average value of 2.38 μBq/kg. The concentration of ^{230}Thxs ranges from 0.8 to 1.7 μBq/kg, with a mean value of 1.37 μBq/kg, except for three sampling sites where no excess ^{230}Thxs was observed.

In the Shaliu River, the concentration of ^{232}Th ranges from 4.488 to 46.913 pmol/kg, with an average of 12.341 pmol/kg, which is higher than that in the Buha River and the Hargai River. The total dissolved ^{230}Th concentration ranges from 3.15 to 39.84 μBq/kg, with an average value of 11.51 μBq/kg. The concentration of ^{230}Thxs ranges from 0.5 to 7.1 μBq/kg with a mean value of 2.89 μBq/kg. The concentrations of ^{232}Th and total dissolved ^{230}Th and ^{230}Thxs of SL-401 are much higher than those in other samples, which may be related to the sampling season. The sample SL-401 was sampled in winter, while other samples were sampled in summer.

In the Hargai River, the concentration of ^{232}Th ranges from 0.433 to 3.132 pmol/kg, with an average value of 1.962 pmol/kg and little variation between sampling sites. The concentration of total dissolved ^{230}Th ranges from 2.62 to 88.41 μBq/kg, with an average value of 31.30 μBq/kg. ^{230}Thxs ranges from 0.4 to 88.1 μBq/kg, with a mean value of 29.93 μBq/kg. HEG-401, which was sampled in winter, had much lower ^{232}Th concentrations than the other two samples. However, the concentration of total dissolved ^{230}Th and ^{230}Thxs of HEG-401 is approximately 40 times and 80 times more than that of the other two samples, respectively.

In the Daotang River, the ^{232}Th concentration ranges from 2.350 to 61.941 pmol/kg, with a mean value of 24.532 pmol/kg. The concentration of total dissolved ^{230}Th ranges from 10.03 to 101.34 μBq/kg, with an average value of 53.78 μBq/kg. The concentration of ^{230}Thxs ranges from 3.5 to 99.7 μBq/kg, with a mean value of 36.6 μBq/kg. There were significant differences in the horizontal distribution of ^{232}Th, total dissolved ^{230}Th, and ^{230}Thxs in the three samples from the Daotang River. The ^{232}Th concentration of DT-401, which was sampled in winter 2020, was 7 times higher than the other samples.

DISCUSSION

Th Scavenging Residence Time in Lake Water

Th Scavenging Residence Time in Surface Lake Water

According to **Equation 1**, we measured the concentration of ^{230}Th at the surface water of Qinghai Lake, determined the ^{230}Th increment generated from ^{234}U decay, and obtained the ^{230}Th residence time (τ_{Th}) in the water column. The details are shown in **Table 4**. The ^{230}Th residence time of surface water samples has a limited variation, ranging from 0.1 to 6.2 years, with an average value of 2.3 years. The concentration of ^{230}Thxs in the southeast lake area is significantly higher than that in the northwest lake area. Thus, the ^{230}Th residence time in the southeast basin is higher than that in the northwest basin, indicating that the particle scavenging rate in the northwest basin is faster than that in the southeast basin, for instance, a slower sedimentation rate in the southeast lake area with ~7-year resolution of deposition recording core in the southeast lake area.

Th Scavenging Residence Time in Depth Profiles of Lake Water

The ^{230}Th concentration differs between stations since the short scavenging residence time of ^{230}Th makes it sensitive to variations in particulate flux (**Figure 2**). The ^{230}Th data show that the residence time of Th in the water column at different depths at 107, which is located in the north of Qinghai Lake, ranges from 1.6 to 4.3 years, with a mean value of 2.8 years and little variation in the vertical profile, indicating that there was

TABLE 4 | Dissolved ^{232}Th concentration, τ_{Th}, dissolved ^{232}Th flux and lithogenic flux of Qinghai Lake.

Sample no,	Depth (m)	Station	Density (kg/M^3)	d^{232}Th (pmol/kg)	τ_{Th} (year)	d^{232}Th Flux (nmol/M^2/yr)	Th-Litho.flux S_{Th} = 1% (g/M^2/yr)	Th-Litho.flux S_{Th} = 10% (g/M^2/yr)
QHH-9-0	0.2	107	1,200	3.356	2.5	0.318	0.70	0.070
QHH-9-3	3			3.097	2.3	4.745	10.48	1.048
QHH-9-6	6			3.815	2.2	12.547	27.72	2.772
QHH-9-9	9			3.381	1.6	22.555	49.84	4.984
QHH-9-12	12			4.885	2.5	28.625	63.25	6.325
QHH-9-15	15			4.046	4.3	17.000	37.56	3.756
QHH-9-18	18			8.978	1.8	106.033	234.28	23.428
QHH-9-21	21			13.229	4.2	78.792	174.09	17.409
QHH-9-24	24			14.995	2.5	171.366	378.64	37.864
QHH-9-27	27			2.941	4.3	22.376	49.44	4.944
QHH-15–0	0.2	123	1,200	0.439	—	—	—	—
QHH-15–3	3			0.544	—	—	—	—
QHH-15–6	6			0.670	—	—	—	—
QHH-15–9	9			0.990	0.3	34.289	75.76	7.576
QHH-15–12	12			0.911	0.5	25.027	55.30	5.530
QHH-15–18	18			1.624	0.2	155.014	342.51	34.251
QHH-15–21	21			1.791	0.7	60.487	133.65	13.365
QHH-15–27	27			1.071	0.2	185.652	410.20	41.020
QHH-21–0	0.2	131	1,200	0.265	4.7	0.013	0.03	0.003
QHH-21–3	3			0.319	6.3	0.182	0.40	0.040
QHH-21–6	6			0.379	3.6	0.766	1.69	0.169
QHH-21–9	9			0.330	4.8	0.736	1.63	0.163
QHH-21–12	12			0.376	4.3	1.256	2.78	0.278
QHH-21–15	15			0.410	2.7	2.690	5.94	0.594
QHH-21–18	18			0.632	2.3	5.811	12.84	1.284
QHH-21–21	21			4.563	4.3	26.840	59.30	5.930
QHH-21–24	24			0.868	3.0	8.341	18.43	1.843
QHH-21–26	26			0.578	4.5	3.969	8.77	0.877
QHH-105-S	0.2	105	1,200	0.560	0.1	1.493	3.30	0.330
QHH-109-S	0.2	109		0.555	3.3	0.040	0.09	0.009
QHH-111-S	0.2	111		0.803	1.9	0.099	0.22	0.022
QHH-113-S	0.2	113		0.500	2.1	0.057	0.13	0.013
QHH-115-S	0.2	115		1.951	3.2	0.146	0.32	0.032
QHH-116-S	0.2	116		3.067	1.1	0.672	1.48	0.148
QHH-118-S	0.2	118		1.735	2.7	0.155	0.34	0.034
QHH-120-S	0.2	120		0.353	1.9	0.043	0.10	0.010
QHH-126-S	0.2	126		0.704	2.1	0.082	0.18	0.018
QHH-127-S	0.2	127		1.195	6.2	0.046	0.10	0.010
QHH-132-S	0.2	132		0.769	3.4	0.055	0.12	0.012
QHH-201-S	0.2	201		2.465	0.1	11.427	25.25	2.525

*The unit of the ^{232}Th residence time obtained in **Eq. 1** is day. This table converts the unit to year for the convenience of discussion.*

no significant difference in the scavenging rate of Th at different depths of the water column in the same area. This likely suggests limited varying particulate matter size and with ~4-year resolution of deposition recording in site 107, which means that it takes ~4 years for particulate matter to be removed from the water column into the sediment. The residence time of Th in site 123 is 0.2–0.7 years, with a mean of 0.4 years, which is lower than that in the other two sites. The ^{230}Th residence time is short and therefore it can be transferred more rapidly from the water column to sinking particulate matter through vertical fluxes, meaning that the scavenging rate is the fastest in the western lake area of Qinghai Lake. This likely suggests a larger particulate matter size with faster removal rates and with ~0.7-year resolution of deposition record in site 123. Site 131 in the southern area of the lake has the longest ^{230}Th residence time varying from 2.3 to 6.3 years, with a mean value of 4.1 years, indicating the slowest scavenging rate in this area. The top depth of site 131 shows a longer residence time, suggesting that there exists another source of older water mixture in the top 10 m and finer particulate size. The relationship between the scavenging rates of the three depth profiles is 123 > 107>131. The variable disequilibrium between the western, northern, and southern regions of the lake area indicates variable and often large particle fluxes and/or changes in particle size from the western lake region rather than the other regions of the lake, which probably indicate more particle matter flux and/or larger particle size from the Buha river mixing into the lake water with hydraulic sorting effect (Tao et al., 2021). Thus, those differences are probably controlled by variations in the river water influx and its corresponding differences in particle flux and/or particle

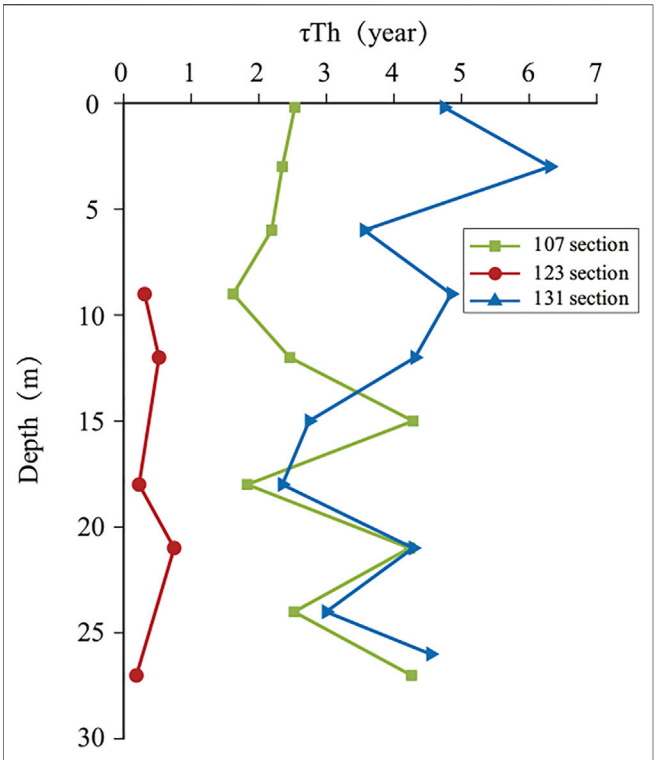

FIGURE 2 | Distribution characteristic of ^{230}Th residence time (τ_{Th}) in depth profiles of Qinghai Lake.

composition in the northern basin and western basin. However, a lower ^{232}Th content in site 131 and a longer residence time indicate a limited effect of the river in the southern basin.

Seasonal Changes in ^{232}Th Content in the Exogenous Rivers of Qinghai Lake

Due to the concentration of ^{232}Th having seasonal differences in lake water, eight samples in different months were selected from four exogenous rivers of Qinghai Lake for analysis and comparison. As shown in **Table 5**, there are visible seasonal changes in the ^{232}Th content of the rivers. The samples from November have higher ^{232}Th concentrations than the June and July samples, except for the Hargai River, where more wetlands and swamps decrease the amount of dust in Hargai during November. Therefore, in the dry season with little wet atmospheric precipitation from October to May, the ^{232}Th content of rivers in the Qinghai region was higher than that in the rainy season from June to September, which was influenced by sand and dust particles from the northwest wind into the lake water.

Thorium-Derived Dissolved ^{232}Th flux and Lithogenic Flux to the Qinghai Lake

Qinghai Lake is a typically closed saline lake, and the lake's recharge water is mainly from exogenous recharge rivers, followed by natural precipitation and groundwater. Previous studies have suggested that the ^{232}Th concentrations in surface water appear to be linked to the water column scavenging rate (Cochran et al., 1995; Edmonds et al., 1998; Edmonds et al., 2004). ^{232}Th is non-radiogenic, so most of the ^{232}Th in the lake water comes from the lake margins (bank erosion), rivers, or aeolian detrital particulate material. Th is insoluble in water and is rapidly eliminated from solution via scavenging on particulate material (Moore and Sackett, 1964). Therefore, if there were no contributions from other sources, the variation of ^{232}Th concentrations in water should decrease with depth and show the highest values in surface water. Therefore, depth profiles can be used to assess the lithogenic fluxes in lake water. More specifically, the ^{232}Th fluxes in deep water indicate a deep source of dissolved ^{232}Th, possibly as a result of boundary scavenging. The sampling profiles indicate that the ^{232}Th concentrations in Qinghai Lake increase slowly with depth, with higher bottom water concentrations in all three profiles. These trends suggest that an additional ^{232}Th enters the water column at the bottom of the lake, possibly from the contribution of the bottom sediments. The ^{232}Th concentrations at the lake surface (**Supplementary Table S1** and **Supplementary Figure S1** in the supplementary material file) suggest that the dissolved ^{232}Th flux is primarily derived from the input of aerosol (dust) in shallow waters. Furthermore, the fluxes near the entrance of the recharging river appear to be derived from the ^{232}Th contributed to the lake by the river. The ^{232}Th in the lake is therefore thought to be due to the dissolution of dust aerosols in combination with inflow from the recharging rivers (Zhang et al., 2019). The characteristics of the horizontal and vertical distribution of ^{232}Th in the lake water of Qinghai Lake suggest that there is an exogenous source contribution, of ^{232}Th to its lake water, and that different areas of the lake do not receive exactly the same proportion of the exogenous source contribution which is from hydraulic sorting of grain size and types. Because several major recharge rivers flow through stratigraphic source rocks that are different, including felsic rocks, carbonate, metamorphic rocks, and clastic rocks. In view of this, it is reasonable to assume that the main sources of ^{232}Th in the lake water column of Qinghai Lake include atmospheric deposition dust, exogenous recharge

TABLE 5 | Seasonal changes of ^{232}Th content in the exogenous rivers of Qinghai Lake.

Sample no.	Latitude (°N) and longitude (°E)	Date	d^{232}Th (pmol/kg)
BH-201	37°22′35″, 98°50′34″	17 June 2018	3.354
BH-301		23 July 2019	1.531
SL-201	37°37′18″, 99°58′17″	18 June 2018	7.976
SL-301		23 July 2019	4.488
SL-401	37°19′92″, 100°07′29″	18 November 2020	46.913
HEG-201	37°17′11″, 100°28′38″	18 June 2018	2.321
HEG-301	37°13′11″, 100°28′37″	23 July 2019	3.132
HEG-401		18 November 2020	0.433
DT-201	36°34′30″, 100°44′49″	19 June 2018	2.35
DT-301		24 July 2019	9.306
DT-401	36°23′56″, 100°58′28″	18 November 2020	61.941

river, and the mix from the interface of water-rock with the water depth increase. Selecting an integration depth at which the lithogenic inputs can be effectively quantified has been a subject of discussion with varying particle types. Due to the sampling method and evaluation method of this study being different from Jin's (Jin et al., 2009a), the lithogenic flux in this study is different from the flux in Jin's. Jin et al. estimated the dust flux based on the suspended particulate matter supplied by the Buha River to Qinghai Lake, and the lithogenic flux of Qinghai Lake in our study includes two sources, atmospheric deposition and river recharge. The dust flux in this study refers to the particulate matter caused by atmospheric dry deposition.

The dissolved ^{232}Th fluxes can be converted to lithogenic-material fluxes with knowledge about the composition of the material and its Th fractional solubility (**Eq. (3)**). In other words, this flux of lithogenic material is required to sustain the calculated dissolved ^{232}Th and therefore the measured concentration of ^{232}Th. The lithogenic material from the Qinghai region has a ^{232}Th content varying from 10.5 to 11.7 μg/g (Wang et al., 2016). Therefore, we use this value for the calculations of the lithogenic flux in our area of study.

The largest source of uncertainty in the calculation of lithogenic fluxes is the solubility of ^{232}Th from particles, which is a highly unconstrained parameter. From the few studies that report ^{232}Th solubility in marine particles, highly variable values were found, ranging from 1% to 23%, depending on the particle size and depth (Arraes-Mescoff et al., 2001; Roy-Barman et al., 2002). There is no report about ^{232}Th solubility in lake particles. According to our preliminary results from lake particles from the Qaidam Basin, ranging from 1 to 10%, depending on the particle size and types (unpublished data).

The Spatial Trends of Dissolved ^{232}Th Flux and Lithogenic Flux in Lake Water

The climatic characteristics of Qinghai Lake do not vary greatly within the region, and the contribution of ^{232}Th atmospheric dust in lake surface water is generally consistent when other exogenous factors are ignored, so the distribution of ^{232}Th concentrations in lake surface water of Qinghai Lake should generally remain consistent under ideal conditions. However, the concentration of ^{232}Th in the surface lake shows that the spatial distribution characteristics of ^{232}Th concentrations in Qinghai Lake vary (0.265–3.356 pmol/kg), with a mean value of 1.24 pmol/kg. Sites 107, 115, 116, 118, and 201, located at the edge of the northwestern lake area, had significantly higher values of ^{232}Th than those in other areas of the lake, with a mean value of 2.513 pmol/kg. The spatial distribution of ^{232}Th concentration in the surface water of Qinghai Lake near the Buha River is significantly higher than that in other areas. The ^{230}Thxs content is significantly higher in the southeast basin than in the northwest basin. The mean value of ^{230}Thxs content at sites 131, 126, 127, and 132 in the south lake is 12.0 μBq/kg, which is much higher than the mean value of surface water, and therefore, exogenous detritus contributes less Th to the south lake area than the other areas.

The results of the dissolved ^{232}Th flux and lithogenic flux in surface lake water were calculated by **equations 2** and **3**. As a study suggested in the Nansen Basin, the Arctic Ocean (Cochran et al. (1995)), elevated particle concentrations near the basin margin, if coupled with greater particle fluxes, could produce enhanced removal of reactive radionuclides from the water column. The dissolved ^{232}Th flux in surface lake water ranges from 0.013 to 26.840 nmol/m^2/yr, with an average value of 5.060 nmol/m^2/yr (**Table 4**; **Figure 3**). The dissolved ^{232}Th flux in the northwest basin has significantly higher values than that in the southeast basin, especially near the entrances of the Buha River and Shaliu River. The results show that in addition to the ^{232}Th contributed by atmospheric deposition, the exogenous recharge rivers contributed a certain amount of ^{232}Th to Qinghai Lake. Sites 105 and 201, located at the northwestern edge of Qinghai Lake, have much shorter Th residence times than average and much higher dissolved ^{232}Th fluxes than other areas, suggesting that the faster rate of particulate matter production in the lake edge area more effectively removes radionuclides, and thus the ^{230}Thxs showed minimal values here.

For lithogenic flux, when using a Th solubility from particles of 1%, we obtain fluxes of lithogenic material ranging from 0.03 to 25.25 g/m^2/yr in the surface water, while the values range from 0.003 to 2.525 g/m^2/yr when using a Th solubility from particles of 10% (**Table 4**; **Figure 4**). It is worth noting that the dissolved ^{232}Th flux and lithogenic flux at site 201 are tens to hundreds of times higher than those of the other sites, which may be due to the sampling location near the lake shore and the source of flux is the dissolution of continental material. Since the lithogenic fluxes in the southeast basin are lower than those in the northwest basin, we believe that the contribution of exogenous detrital materials by river input to lake water in the southern basin is limited. The dust flux in September from atmospheric deposition can thus be confirmed. In general, when other exogenous factors are ignored, the dust flux from Qinghai Lake in September is basically stable with a value of 0.109 g/m^2/yr.

The Depth Trends of Dissolved ^{232}Th Flux and Lithogenic Flux in Lake Water

The mixing of runoff from exogenous recharge rivers with the original water of Qinghai Lake may affect the variation of ^{232}Th flux and lithogenic flux in the lake water column and eventually affect the vertical distribution of ^{232}Th concentration in the lake water. The distribution characteristics of ^{232}Th concentration in the lake water column with vertical gradient and the residence time of Th in the water column combined with **Eq. 2** and **Eq. 3** calculated the vertical gradient profile flux. The calculation results are shown in **Table 4**. Dissolved ^{232}Th flux and lithogenic flux in all three depth profiles of Qinghai Lake showed an increasing trend with depth (**Figure 5**, **Figure 6**). Site 107, located northwest of the lake, has the highest dissolved ^{232}Th flux and a higher mean particulate flux. This site has the largest increase in dissolved ^{232}Th flux, which ranges from 0.318 to 171.366 nmol/m^2/yr from the lake surface to the bottom, with a mean value of 46.436 nmol/m^2/yr. The lithogenic flux of site 107 varied from 0.7 to 378.64 g/m^2/yr, with an average value of 102.60 g/m^2/yr. The dissolved ^{232}Th flux and lithogenic flux at site 123 near the center of the lake also increased with depth, peaking at the highest mean values of 57.56 nmol/m^2/yr and 127.18 g/m^2/yr, respectively. Site 131,

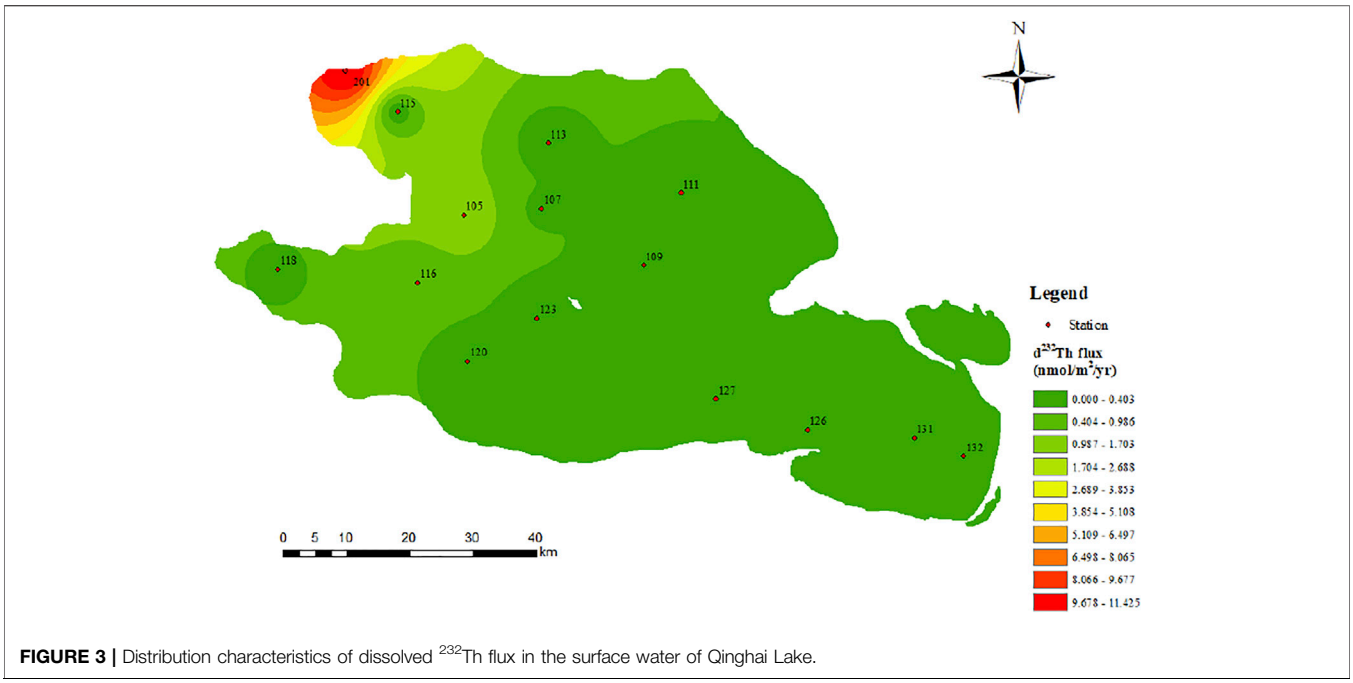

FIGURE 3 | Distribution characteristics of dissolved ^{232}Th flux in the surface water of Qinghai Lake.

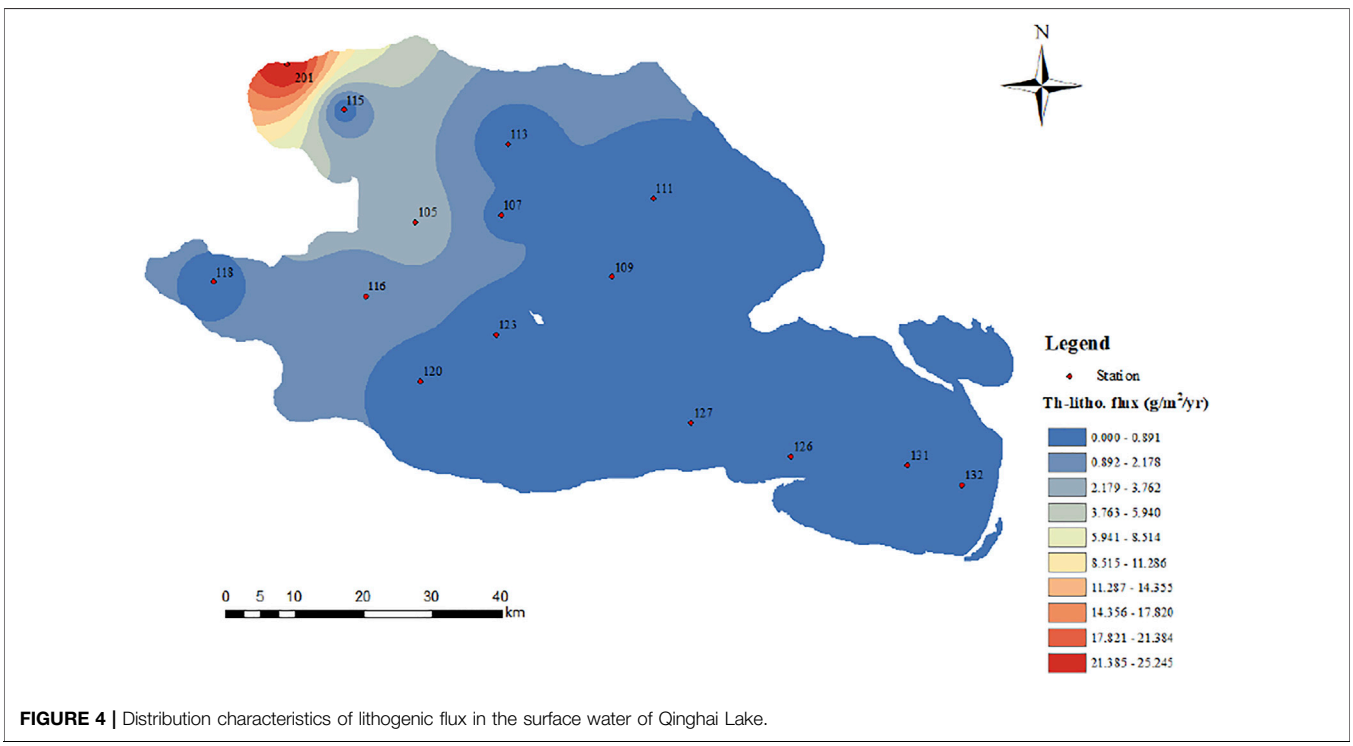

FIGURE 4 | Distribution characteristics of lithogenic flux in the surface water of Qinghai Lake.

located in the south area of Qinghai Lake, has the least dissolved ^{232}Th flux and lithogenic flux. The dissolved ^{232}Th flux ranges from 0.013 to 26.840 nmol/m^2/yr, with an average value of 5.060 nmol/m^2/yr. The lithogenic flux of site 131 ranges from 0.03 to 59.30 g/m^2/yr, with an average value of 11.18 g/m^2/yr. The data from three depth profiles in Qinghai Lake show that dissolved ^{232}Th flux and lithogenic flux increase with depth, and the average dissolved ^{232}Th flux and lithogenic flux in the northwest basin is significantly higher than that in the southeast basin, which has a great relationship with the input of the exogenous recharge river and hydraulic sorting.

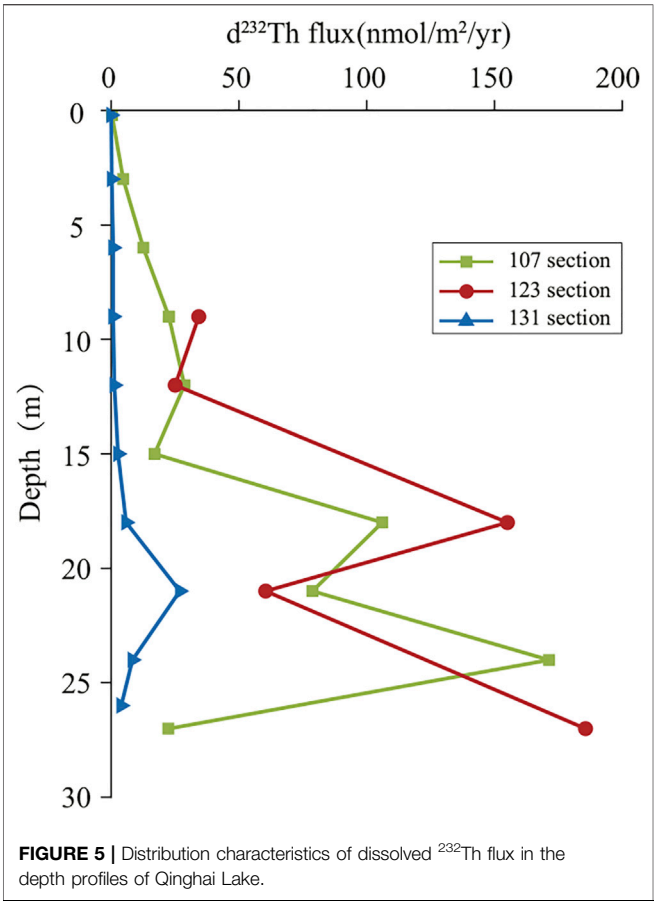

FIGURE 5 | Distribution characteristics of dissolved ^{232}Th flux in the depth profiles of Qinghai Lake.

In the three depth profiles of Qinghai Lake, sites 107, 123, and 131, total dissolved ^{230}Th and ^{230}Thxs showed an increasing trend only at sites 107 and 123, which is similar to the trend of positive correlation of ^{230}Th with water depth in marine water (Cochran et al., 1995). In contrast, ^{230}Thxs shows a decreasing trend at site 131, in complete contradiction to the linear increase in ^{230}Th content in marine water with water depth, which is probably from the mixing of other older water sources. The ^{230}Thxs values are higher than those in the northwest lake area. When the parent nuclide of ^{230}Th, ^{234}U, is approximately homogeneous in the lake water, combined with the lower contribution of ^{232}Th and ^{230}Th from exogenous particulate matter, it can be assumed that the scavenging rate at site 131 was slower. In addition, it has been shown that the nature of the particulate matter plays a role in the removal effect of ^{230}Th in the lake (Clegg and Whitfield, 1991). The mean particulate matter flux at depth profile 131 is approximately ten times lower than that at the other two sites, and the mean ^{232}Th concentration is the lowest of the three sites. Since site 131 is away from the Daotang River, which first flows into Erhai, then flows into Qinghai Lake through a limited channel, the recharge water from Erhai is characterized by low fluxes and higher Th concentrations. It can be inferred that the Daotang River and Erhai contribute very limited exogenous particulate matter to the south of Qinghai Lake and that the source of particulate matter in the southeastern lake area of Qinghai Lake is mainly the dissolution of atmospheric dust with low content ^{232}Th contribution to the lake surface water. Since there is a bird island in the center of the lake, and combined with the fact that the lithologic fluxes based on ^{232} Th decrease sequentially from northwest to southeast in the surface layer, the surface fluxes located at the south of the bird island do not show a decreasing gradient in contrast to the north, we believe that there exists a limited possibility of river transpolar to the southeast.

Quantification of Lithogenic Fluxes to the Qinghai Lake Based on the Mixing of River in Lake Water

As the two largest recharge rivers to Qinghai Lake, both the Buha River and the Shaliu River have higher mean values of ^{232}Th concentrations than those in the surface water of Qinghai Lake (mean value of 1.247 pmol/kg). The high values of ^{232}Th combined with the low values of ^{230}Thxs indicate that these two rivers carry more exogenous debris material and contribute a certain amount of particulate matter to the lake. Thus, the high values of ^{232}Th at sites near the northwestern edge of Qinghai Lake (107, 115, 116, 118, and 201) suggest that the inputs from the Buha River and the Shaliu River may be responsible for this phenomenon. The low values of ^{232}Th near the river entrances of the Hargai and Daotang Rivers show that these two rivers contribute limited flux to the lake.

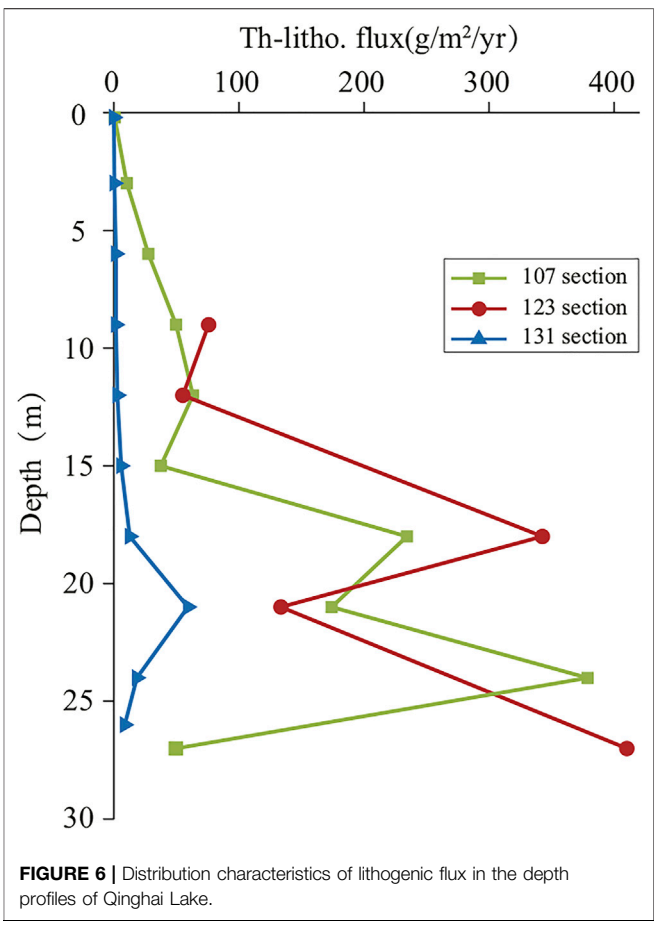

FIGURE 6 | Distribution characteristics of lithogenic flux in the depth profiles of Qinghai Lake.

TABLE 6 | Comparison of lithogenic flux in the present study with the results of sediments from the study of Jin et al. (2013).

Area of study		Th-Litho.flux S_{Th} = 1% (g/M^2/yr)	Th-Litho.flux S_{Th} = 10% (g/M^2/yr)	Fluxes of settled particles (g/M^2/yr)	
				2010.7–2010.12	2011.1–2011.10
Northwest basin of Qinghai Lake	Surface water	0.09–25.25	0.009–2.525	—	—
	Depth profiles	0.70–410.20	0.070–4.102	—	—
Southeast basin of Qinghai Lake	Surface water	0.03–1.48	0.003–0.148	-—	—
	Depth profiles	0.03–59.30	0.003–5.930	—	—
Qinghai Lake*	Rainy season	—	—	13.25–723.54	12.59–99.57
	Dry season	—	—	6.57–387.81	1.02–13.18

**Fluxes of settled particles data of Qinghai Lake is from Jin et al. (2013).*

Previous studies have shown that the uranium content in Qinghai Lake shows a uniform distribution, indicating that its activity is generally consistent, which implies that there is always a consistent and steady-state source of ^{230}Thxs in the lake water (Zhang et al., 2019). However, the determination of thorium isotopes at each station in Qinghai Lake revealed that the content varies greatly from station to station, which is very different from the distribution of uranium isotopes in the lake water. Due to the pro-particulate properties of thorium (Kretschmer et al., 2010), thorium is easily eliminated by the migration and removal of particulate materials. Therefore, the horizontal river and the amount of particulate material have a huge influence on it.

We compared the lithogenic flux of surface water and depth profiles of Qinghai Lake with the results of Qinghai Lake sediments in the study of Jin et al. (2013), and the results were consistent (**Table 6**). Thus, the lithogenic material flux calculation using thorium isotopes for the QHH region seems to be promising, and once the Th solubility in the QHH lake is better constrained, the uncertainties will be reduced. The long-lived Th isotopes offer a unique and powerful tool to evaluate the supply of lithogenic flux. However, there are a number of sources of uncertainty that must be addressed in future studies to further refine our estimates of lithogenic fluxes. These include seasonal effects of Th input and removal in the lake away from the edge of QHH, the chemical speciation and size partitioning of ^{232}Th and ^{230}Th in lake water.

In conclusion, when a large number of exogenous recharge rivers are mixed into the northwest basin of Qinghai Lake, the ^{232}Th content and lithogenic flux of the lake water are mainly influenced by the type and content of the particles in the Buha and Shaliu rivers. Conversely, when the contribution of recharge rivers is limited, the ^{232}Th content of the lake water is mainly influenced by atmospheric dust. For example, based on the ^{230}Th normalization method (combining with ^{232}Th and τ_{Th}), the dust flux in September can be evaluated. Based on the safety of sampling on the lake, the samples were collected at a time when there was no wind and no rain. Thus, the atmospheric dust could be evaluated. And based on the retention time of particulate matter in the water column, the depth profile results can reflect the lithogenic fluxes on a seasonal to annual scale with some certainty.

Contribution of Recharging Rivers of Qinghai Lake and Atmospheric Dust to ^{232}Th Fluxes in Lake Water Column

According to previous studies (Edmonds et al., 1998; Edmonds et al., 2004; Hayes et al., 2017), since most of the dissolved ^{232}Th in seawater originates from atmospheric dust which dissolves into the ocean after settling to the sea surface, the ^{232}Th concentration in marine waters decreases with depth and reaches its highest value at the sea surface. This is in contrast to the phenomenon we observed in the lake. All three depth profiles of Qinghai Lake showed a positive correlation between ^{232}Th concentration and depth, and the high ^{232}Th values in surface waters near site 107 suggested that this may be due to the input from exogenous recharge rivers. The advection of particulate matter from the nearshore shelf can increase regional scavenging rates and fluxes. The recharge rivers carried more exogenous detrital material into the lake and mixed it with the lake water, causing the particulate flux to increase with depth and reaching a maximum in the bottom water of the lake.

Based on Th isotope data and flux information of surface water in Qinghai Lake, the dust flux of lithologic material in September contributed by atmospheric dry deposition to the lake can be calculated, which is approximately 0.109 g/m^2/yr. The lithogenic fluxes delivered to the lake by rivers can be quantified based on the data from stations located near the recharging rivers. The fluxes of lithologic material from the recharge rivers input into the lake are 120.55 g/m^2/yr in the northwest basin and 12.42 g/m^2/yr in the southeast basin, which are calculated by the mean value of lithogenic fluxes at depth profiles of 107 and 123 sites and the mean value at depth profile site 131, respectively. Sites 126, 127, 131, and 132 are located in the southeast of Qinghai Lake, far away from the estuary, and the ^{232}Th of surface water is mainly derived from atmospheric dust. The mean lithogenic flux of the surface water at these four sites is 0.109 g/m^2/yr. Sites 105, 107, 113, 115, 116, and 118 are located in the northwest and southwest of Qinghai Lake near the estuary. Their lithogenic fluxes mainly come from fluvial suspended particles and atmospheric dust. The mean lithogenic flux of the surface water at these six sites is 1.046 g/m^2/yr. The contribution of atmospheric dust and river input to the lithogenic flux of Qinghai Lake can be assessed by these two mean values. For instance, the Buha River and Shaliu River contribute ~90% of the lithogenic flux to the northwest

basin of the lake, while the atmospheric dry dust deposition contributes only 10% of the flux. Therefore, unlike the northwest region, the source of particle material flux in the southeast basin of the lake is dominated by atmospheric deposition, and the contribution of the recharging river to the lake's water flux is less than that of the atmospheric dissolution of dust at the lake surface. In jin et al. (2009a), the dust input represents 65% of the total input of dissolved and particulate forms, which is estimated based on the suspended particulate matter supplied by the Buha River to Qinghai Lake. Among the four recharge rivers of Qinghai Lake, from our result, the Buha and Shaliu Rivers have higher lithogenic fluxes, including dust input into the river and ^{232}Th concentrations, contributing a large amount of particulate matter to the northwestern area of Qinghai Lake with a ratio of ~90% of the detrital flux to the lake in September, which is actually not contradictory to Jin's result with ~65% of the dust input origin of the total input of dissolved and particulate forms in the Buha River and recharge into Qinghai Lake. This study supplies several rivers' loads into the lake by a novel ^{230}Th normalization method, which is further complementary to the detrital flux into Qinghai Lake with several major incharge rivers.

Hayes et al. (2013) suggest that there are two sources of Th in the ocean: one shallow due to dust dissolution and one deep associated with sediment dissolution/resuspension; and one removal mechanism, scavenging throughout the water column. Therefore, another reason for the higher concentration of ^{232}Th in the deep water than in the surface water in the saline lakes may be due to the redissolution of ^{232}Th in the sediment at the bottom of the lake. The other possibility is from accumulated sinking flux due to the slow deposition rate. In the future, we expect to use Th isotope information in lake sediments, combined with Th concentration data of depth profile particles' composition and size, to further quantify the contribution of ^{232}Th to lake sediments.

Overall, in September, the Buha and Shaliu rivers in the northwest basin contribute about 90% of the detrital ^{232}Th flux to the lake. The lithogenic flux in the southeast lake is dominated by dust flux with a value of ~0.109 g/m^2/yr, while the higher lithogenic flux at the bottom of the lake was likely generated by accumulated sinking particulate matter and resuspension of bottom sediments in September.

CONCLUSION

The ^{232}Th concentrations on the horizontal spatial scale at the surface of Qinghai Lake are unevenly distributed, being significantly higher around the river entrance of the northwest basin than in other lake areas, with more ^{230}Th from exogenous material in the total dissolved water. When a large number of exogenous recharge rivers are mixed into the lake water in the northwest basin, the ^{232}Th content and the corresponding dust flux of the lake water are mainly influenced by the type and content of the recharging river particles. Conversely, when the recharge river contribution is limited in the southeast basin, the ^{232}Th content of the lake water away from the estuary is mainly influenced by the atmospheric dust. Furthermore, based on the ^{230}Th normalization method (combining with ^{232}Th and τ_{Th}), the dust flux of Qinghai Lake in September can be evaluated with an average of ~0.109 g/m^2/yr. When using a Th solubility from particles of 1%, the fluxes of lithogenic material range from 0.03 to 25.25 g/m^2/yr in the surface water, consistent with the flux results of settled particles from the previous study. Deposition record resolutions of 7, 4, and 0.7 years are present in the southeast, northwest, and southwest of Qinghai Lake, respectively.

Among the four recharge rivers of Qinghai Lake, the Buha and Shaliu rivers have higher ^{232}Th concentrations, contributing a large amount of particulate matter to the northwestern area of Qinghai Lake, with a ratio of ~90% of the detrital flux to the lake in September. The lithogenic flux in the southeast lake is dominated by dust flux with a value of ~0.109 g/m^2/yr, while the higher lithogenic flux at the bottom of the lake was likely generated by accumulated sinking particulate matter and resuspension of bottom sediments in September. This study confirms the utility of long-lived Th isotopes to quantify lithogenic inputs based on the Th content of the dissolved lake water and also supply deposition resolution information for QHH sediment records with some certainty.

DATA AVAILABILITY STATEMENT

The original contributions presented in the study are included in the article/**Supplementary Material**; further inquiries can be directed to the corresponding authors.

AUTHOR CONTRIBUTIONS

The research was supervised by PZ and XL, with guidance provided by RE. Samples were collected by PZ, XP, CC, JP, LL, and XL. The experiment method was instructed by PZ, CC, ZG, XL, and YN. The manuscript was written by PZ with revisions provided by LT, XL, and RE. All authors have read and agreed to the published version of the manuscript.

FUNDING

This study was supported by the National Natural Science Foundation of China (Nos. 41873013 and 41888101) and the U.S. NSF (No. 1702816).

SUPPLEMENTARY MATERIAL

The Supplementary Material for this article can be found online at: https://www.frontiersin.org/articles/10.3389/feart.2022.866314/full#supplementary-material

REFERENCES

Ankney, M., Bacon, C., Valley, J., Beard, B., and Johnson, C. (2017). Oxygen and U-Th Isotopes and the Timescales of Hydrothermal Exchange and Melting in Granitoid wall Rocks at Mount Mazama, Crater Lake, Oregon. *Geochimica et Cosmochimica Acta* 213, 137–154. doi:10.1016/j.gca.2017.04.043

Arraes-Mescoff, R., Roy-Barman, M., Coppola, L., Souhaut, M., Tachikawa, K., Jeandel, C., et al. (2001). The Behavior of Al, Mn, Ba, Sr, REE and Th Isotopes during *In Vitro* Degradation of Large marine Particles. *Mar. Chem.* 73 (1), 1–19. doi:10.1016/s0304-4203(00)00065-7

Bacon, M. P. (1984). Glacial to Interglacial Changes in Carbonate and clay Sedimentation in the Atlantic Ocean Estimated from 230Th Measurements. *Chem. Geology*. 46 (2), 97–111. doi:10.1016/0009-2541(84)90183-9

Bian, Q., Liu, J., Luo, X., Xiao, J., Ritzwoller, M., and Levshin, A. (2000). Geotectonic Setting, Formation and Evolution of the Qinghai Lake. *Ssmology Geology*. 22 (1), 20–26. (in Chinese). doi:10.3969/j.issn.0253-4967.2000.01.003

Bourdon, B., Turner, S., and Dosseto, A. (2003). Dehydration and Partial Melting in Subduction Zones: Constraints from U-Series Disequilibria. *J. Geophys. Res.* 108 (B6), 2291. doi:10.1029/2002jb001839

Cheng, H., Edwards, R.L., Hoff, J., Gallup, C.D., Richards, D. A., and Asmerom, Y. (2000). The Half-Lives of Uranium-234 and Thorium-230. *Chem. Geology*. 169 (1-2), 17–33. doi:10.1016/s0009-2541(99)00157-6

Cheng, H., Lawrence Edwards, R., Shen, C.-C., Polyak, V. J., Asmerom, Y., Woodhead, J., et al. (2013). Improvements in 230Th Dating, 230Th and 234U Half-Life Values, and U-Th Isotopic Measurements by Multi-Collector Inductively Coupled Plasma Mass Spectrometry. *Earth Planet. Sci. Lett.* 371-372, 82–91. doi:10.1016/j.epsl.2013.04.006

Clegg, S. L., and Whitfield, M. (1991). A Generalized Model for the Scavenging of Trace Metals in the Open Ocean-II. Thorium Scavenging. *Deep Sea Res. A. Oceanographic Res. Pap.* 38 (1), 91–120. doi:10.1016/0198-0149(91)90056-l

Cochran, J. K., Hirschberg, D. J., Livingston, H. D., Buesseler, K. O., and Robert, M. K. (1995). Natural and Anthropogenic Radionuclide Distributions in the Nansen Basin, Artic Ocean: Scavenging Rates and Circulation Timescales. *Topical Stud. Oceanography* 42 (95), 1495–1517. doi:10.1016/0967-0645(95)00051-8

Colman, S. M., Yu, S. Y., An, Z., Shen, J., and Henderson, A. C. G. (2007). Late Cenozoic Climate Changes in China's Western interior: A Review of Research on lake Qinghai and Comparison with Other Records. *Quat. Sci. Rev.* 26 (2007), 2281–2300. doi:10.1016/j.quascirev.2007.05.002

Costa, K., and McManus, J. (2017). Efficacy of 230Th normalization in sediments from the Juan de Fuca Ridge, northeast Pacific Ocean. *Geochimica et Cosmochimica Acta* 197, 215–225. doi:10.1016/j.gca.2016.10.034

Cruz, J. A., McDermott, F., Turrero, M. J., Edwards, R. L., and Martin-Chivelet, J. (2021). Strong Links between Saharan Dust Fluxes, Monsoon Strength, and North Atlantic Climate during the Last 5000 Years. *Sci. Adv.* 7 (26), eabe6102. doi:10.1126/sciadv.abe6102

Curry, W. B., and Lohmann, G. P. (1986). Late Quaternary Carbonate Sedimentation at the Sierra Leone Rise (Eastern Equatorial Atlantic Ocean). *Mar. Geology*. 70, 223–250. doi:10.1016/0025-3227(86)90004-6

DeMaster, D. J. (1981). The Supply and Accumulation of Silica in the marine Environment. *Geochimica et Cosmochimica Acta* 45 (10), 1715–1732. doi:10.1016/0016-7037(81)90006-5

Ding, Y. H., Li, Q. P., Liu, Y. J., Zhang, L., Song, Y. F., and Zhang, J. (2009). Air Pollution and Climate Change. *Meteorology* 035 (003), 3–14. (in Chinese).

Edmonds, H. N., Moran, S. B., Hai, C., and Edwards, R. L. (2004). ^{230}Th and 231Pa in the Arctic Ocean: Implications for Particle Fluxes and basin-scale Th/Pa Fractionation. *Earth Planet. Sci. Lett.* 227 (1-2), 155–167. doi:10.1016/j.epsl.2004.08.008

Edmonds, H. N., Moran, S. B., Smith, J. A. J. N., and Edwards, R. L. (1998). Protactinium-231 and Thorium-230 Abundances and High Scavenging Rates in the Western Arctic Ocean. *Science* 280 (5362), 405–407. doi:10.1126/science.280.5362.405

Francois, R., Frank, M., Loeff, M. R., and Bacon, M. (2004). ^{230}Th Normalization: An Essential Tool for Interpreting Sedimentary Fluxes during the Late Quaternary. *Paleoceanography* 19, 1018. doi:10.1029/2003pa000939

Hayes, C. T., Anderson, R. F., Fleisher, M. Q., Serno, S., Winckler, G., and Gersonde, R. (2013). Quantifying Lithogenic Inputs to the North Pacific Ocean Using the Long-Lived Thorium Isotopes. *Earth Planet. Sci. Lett.* 383 (383), 16–25. doi:10.1016/j.epsl.2013.09.025

Hayes, C. T., Rosen, J., Mcgee, D., and Boyle, E. A. (2017). Thorium Distributions in High- and Low-dust Regions and the Significance for Iron Supply. *Glob. Biogeochem. Cycles* 31 (2), 328–347. doi:10.1002/2016gb005511

Jickells, T. D., An, Z. S., Andersen, K. K., Baker, A. R., Bergametti, G., Brooks, N., et al. (2005). Global Iron Connections between Desert Dust, Ocean Biogeochemistry, and Climate. *Science* 308 (5718), 67–71. doi:10.1126/science.1105959

Jin, Z. D., Zhang, F., Li, F. C., Chen, L. M., Xiao, J., and He, M. Y. (2013). Seasonal and Interannual Variations of the lake Water Parameters and Particle Flux in Lake Qinghai: A Time-Series Sediment Trap Study. *J. Earth Environ.* 4 (3), 8. (in Chinese).

Jin, Z., You, C.-F., and Yu, J. (2009a). Toward a Geochemical Mass Balance of Major Elements in Lake Qinghai, NE Tibetan Plateau: A Significant Role of Atmospheric Deposition. *Appl. Geochem.* 24 (10), 1901–1907. doi:10.1016/j.apgeochem.2009.07.003

Jin, Z., You, C.-F., Yu, T.-L., and Wang, B.-S. (2010). Sources and Flux of Trace Elements in River Water Collected from the Lake Qinghai Catchment, NE Tibetan Plateau. *Appl. Geochem.* 25 (10), 1536–1546. doi:10.1016/j.apgeochem.2010.08.004

Jin, Z., Yu, J., Wang, S., Zhang, F., Shi, Y., and You, C.-F. (2009b). Constraints on Water Chemistry by Chemical Weathering in the Lake Qinghai Catchment, Northeastern Tibetan Plateau (China): Clues from Sr and its Isotopic Geochemistry. *Hydrogeol J.* 17 (8), 2037–2048. doi:10.1007/s10040-009-0480-9

Kretschmer, S., Geibert, W., Loeff, M., and Mollenhauer, G. (2010). Grain Size Effects on ^{230}Thxs Inventories in Opal-Rich and Carbonate-Rich marine Sediments. *Earth Planet. Sci. Lett.* 294 (1-2), 131–142. doi:10.1016/j.epsl.2010.03.021

Krishnaswami, S., and Cochran, J. K. (2016). Uranium-Thorium Radionuclides in Ocean Profiles. *Encyclopedia Ocean Sci.* 1, 377–391. doi:10.1016/b978-0-12-409548-9.09760-8

Li, X.-Y., Xu, H.-Y., Sun, Y.-L., Zhang, D.-S., and Yang, Z.-P. (2007). Lake-level Change and Water Balance Analysis at Lake Qinghai, West China during Recent Decades. *Water Resour. Manage.* 21 (9), 1505–1516. doi:10.1007/s11269-006-9096-1

Lyle, M., Murray, D. W., Finney, B. P., Dymond, J., Robbins, J. M., and Brooksforce, K. (1988). The Record of Late Pleistocene Biogenic Sedimentation in the Eastern Tropical Pacific Ocean. *Paleoceanography* 3 (1), 39–59. doi:10.1029/pa003i001p00039

Lyle, M. W., and Dymond, J. (1976). Metal Accumulation Rates in the Southeast pacific - Errors Introduced from Assumed Bulk Densities. *Earth Planet. Sci. Lett.* 30 (2), 164–168. doi:10.1016/0012-821x(76)90242-9

Marcantonio, F., Anderson, R. F., Stute, M., Kumar, N., Schlosser, P., and Mix, A. (1996). Extraterrestrial 3He as a Tracer of marine Sediment Transport and Accumulation. *Nature* 383 (6602), 705–707. doi:10.1038/383705a0

Martin, J. H., and Fitzwater, S. E. (1988). Iron Deficiency Limits Phytoplankton Growth in the north-east Pacific Subarctic. *Nature* 331 (6154), 341–343. doi:10.1038/331341a0

McGee, D., and Mukhopadhyay, S. (2013). Extraterrestrial He in Sediments: From Recorder of Asteroid Collisions to Timekeeper of Global Environmental Changes. *The Noble Gases Geochem. Trac.*, 155–176. doi:10.1007/978-3-642-28836-4_7

Moore, W. S., and Sackett, W. M. (1964). Uranium and Thorium Series Inequilibrium in Sea Water. *J. Geophys. Res.* 69 (24). doi:10.1029/jz069i024p05401

Mortlock, R. A., Charles, C. D., Froelich, P. N., Zibello, M. A., Saltzman, J., Hays, J. D., et al. (1991). Evidence for Lower Productivity in the Antarctic Ocean during the Last Glaciation. *Nature* 351, 220–223. doi:10.1038/351220a0

Ojovan, M. I., and Lee, W. E. (2014). "Naturally Occurring Radionuclides," in *An Introduction to Nuclear Waste Immobilisation*. (Oxford: Elsevier), 31–39. doi:10.1016/b978-0-08-099392-8.00004-8

Rea, D. K., and Leinen, M. (1988). Asian Aridity and the Zonal Westerlies: Late Pleistocene and Holocene Record of Eolian Deposition in the Northwest Pacific

Ocean. *Palaeogeogr. Palaeoclimatol. Palaeoecol.* 66, 1–8. doi:10.1016/0031-0182(88)90076-4

Roy-Barman, M., Coppola, L., and Souhaut, M. (2002). Thorium Isotopes in the Western Mediterranean Sea: an Insight into the marine Particle Dynamics. *Earth Planet. Sci. Lett.* 196 (3-4), 161–174. doi:10.1016/s0012-821x(01)00606-9

Roy-Barman, M., LemaïTre, C., Ayrault, S., Jeandel, C., Souhaut, M., and Miquel, J. C. (2009). The Influence of Particle Composition on Thorium Scavenging in the Mediterranean Sea. *Earth Planet. Sci. Lett.* 286 (3-4), 526–534. doi:10.1016/j.epsl.2009.07.018

Santschi, P. H., Murray, J. W., Baskaran, M., Benitez-Nelson, C. R., Guo, L. D., Hung, C.-C., et al. (2006). Thorium Speciation in Seawater. *Mar. Chem.* 100, 250–268. doi:10.1016/j.marchem.2005.10.024

Sarnthein, M., Winn, K., Duplessy, J.-C., and Fontugne, M. R. (1988). Global Variations of Surface Ocean Productivity in Low and Mid Latitudes: Influence on CO2reservoirs of the Deep Ocean and Atmosphere during the Last 21,000 Years. *Paleoceanography* 3, 361–399. doi:10.1029/pa003i003p00361

Shen, C.-C., Wu, C.-C., Cheng, H., Lawrence Edwards, R., Hsieh, Y.-T., Gallet, S., et al. (2012). High-precision and High-Resolution Carbonate 230Th Dating by MC-ICP-MS with SEM Protocols. *Geochimica et Cosmochimica Acta* 99, 71–86. doi:10.1016/j.gca.2012.09.018

Shen, C. C., Edwards, R. L., Cheng, H., Dorale, J. A., Thomas, R. B., Moran, S. B., et al. (2002). Uranium and Thorium Isotopic and Concentration Measurements by Magnetic Sector Inductively Coupled Plasma Mass Spectrometry. *Chem. Geology.* 185 (3), 165–178. doi:10.1016/s0009-2541(01)00404-1

Tao, H., Hao, L., Li, S., Wu, T., Qin, Z., and Qiu, J. (2021). Geochemistry and Petrography of the Sediments from the Marginal Areas of Qinghai Lake, Northern Tibet Plateau, China: Implications for Weathering and Provenance. *Front. Earth Sci.* 9. doi:10.3389/feart.2021.725553

Wan, D., Jin, Z., and Wang, Y. (2012). Geochemistry of Eolian Dust and its Elemental Contribution to Lake Qinghai Sediment. *Appl. Geochem.* 27 (8), 1546–1555. doi:10.1016/j.apgeochem.2012.03.009

Wang, X. Q., Zhou, J., Xu, S. F., Chi, Q. H., Nie, L. S., Zhang, B. M., et al. (2016). China Soil Geochemical Baselines Networks: Data Characteristics. *Geology. China* 43 (5), 12. (in Chinese). doi:10.12029/gc20160501

Winckler, G., Anderson, R. F., Stute, M., and Schlosser, P. (2004). Does Interplanetary Dust Control 100 Kyr Glacial Cycles? *Quat. Sci. Rev.* 23 (18-19), 1873–1878. doi:10.1016/j.quascirev.2004.05.007

Xu, H., Liu, X., An, Z., Hou, Z., Dong, J., and Liu, B. (2010). Spatial Pattern of Modern Sedimentation Rate of Qinghai Lake and a Preliminary Estimate of the Sediment Flux. *Chin. Sci. Bull.* 55, 621–627. doi:10.1007/s11434-009-0580-x

Zhang, F., Jin, Z., Hu, G., Li, F., and Shi, Y. (2009). Seasonally Chemical Weathering and CO2 Consumption Flux of Lake Qinghai River System in the Northeastern Tibetan Plateau. *Environ. Earth Sci.* 59 (2), 297–313. doi:10.1007/s12665-009-0027-3

Zhang, P., Cao, C. Y., Li, X. Z., Pei, X. Z., Chen, C., Liang, L. H., et al. (2021). Effects of Ice Freeze-Thaw Processes on U Isotope Compositions in saline Lakes and Their Potential Environmental Implications. *Front. Earth Sci.* 9, 1143. doi:10.3389/feart.2021.779954

Zhang, P., Cheng, H., Liu, W. G., Mo, L. T., Li, X. Z., Ning, Y. F., et al. (2019). Geochemical and Isotopic (U, Th) Variations in lake Waters in the Qinghai Lake Basin, Northeast Qinghai-Tibet Plateau, China: Origin and Paleoenvironmental Implications. *Arabian J. Geosciences* 12 (92). doi:10.1007/s12517-019-4255-x

Zhang, P. X., Zhang, B. Z., Qian, G. M., Li, H. J., and Xu, L. M. (1994). The Study of Paleoclimatic Parameter of Qinghai Lake since Holocene. *Quat. Sci.* 14 (3), 225–238.

Zhang, X. Y., Arimoto, R., and An, Z. S. (1997). Dust Emission from Chinese Desert Sources Linked to Variations in Atmospheric Circulation. *J. Geophys. Res.* 102 (D23), 28041–28047. doi:10.1029/97jd02300

Zhao, C., Zhang, P., Li, X., Ning, Y., Tan, L., Edwards, R. L., et al. (2020). Distribution Characteristics and Influencing Factors of Uranium Isotopes in saline lake Waters in the Northeast of Qaidam Basin. *Minerals* 10 (1), 74. doi:10.3390/min10010074

Conflict of Interest: The authors declare that the research was conducted in the absence of any commercial or financial relationships that could be construed as a potential conflict of interest.

Publisher's Note: All claims expressed in this article are solely those of the authors and do not necessarily represent those of their affiliated organizations, or those of the publisher, the editors, and the reviewers. Any product that may be evaluated in this article, or claim that may be made by its manufacturer, is not guaranteed or endorsed by the publisher.